



ChemComm

Ligand Non-Innocence Allows Isolation of a Neutral and Terminal Niobium Nitride

Journal:	<i>ChemComm</i>
Manuscript ID	CC-COM-08-2022-004696.R1
Article Type:	Communication

SCHOLARONE™
Manuscripts

Ligand Non-Innocence Allows Isolation of a Neutral and Terminal Niobium Nitride

Received 00th January 20xx,
Accepted 00th January 20xx

Shuruthi Senthil,^a Seongyeon Kwon,^{b,c} Hoyoung Lim,^{b,c} Michael R. Gau,^a Mu-Hyun Baik,^{*c,b} and Daniel J. Mindiola^{*a}

DOI: 10.1039/x0xx00000x

www.rsc.org/

Complex $(\text{PNP})\text{NbCl}_2(\text{N}^t\text{BuAr})$ (**1**) ($\text{PNP}^- = \text{N}[\text{2-}i\text{Pr}_2\text{-4-methylphenyl}]_2$; $\text{Ar} = \text{3,5-Me}_2\text{C}_6\text{H}_3$) reacts with one equiv of NaN_3 to form a mixture of $(\text{PNPN})\text{NbCl}_2(\text{N}^t\text{BuAr})$ (**2**) and $(\text{PNP})\text{Nb}\equiv\text{N}(\text{N}^t\text{BuAr})$ (**3**), both of which have been spectroscopically and crystallographically characterized, including ^{15}N isotopic labelling studies. Complex **3** represents the first structurally characterized example of a neutral and mononuclear Nb nitride. Independent studies established **3** to form via two-electron reduction of **2**, whereas oxidation of **3** by two-electrons reversed the process. Computational studies suggest the transmetalation step to produce the intermediate $[(\text{PNP})\text{NbCl}(\text{N}_3)(\text{N}^t\text{BuAr})]$ (**A**) which extrudes N_2 to form the phosphinimide $[(\text{PNPN})\text{NbCl}(\text{N}^t\text{BuAr})]$ (**B**) followed by disproportionation to **2** and low-valent $[(\text{PNPN})\text{Nb}(\text{N}^t\text{BuAr})]$ (**C**). The latter then undergoes intramolecular N-atom transfer to form the nitride moiety in **3**.

Although niobium nitride (NbN) has found widespread use as a thermally robust superconducting thin film in electronic devices¹⁻⁴ and as supercapacitors,^{5, 6} little is known about the nature of the NbN functionality. One approach is to prepare discrete monomers having this functional group on Nb,⁷⁻¹⁰ but given the high charge of N^{3-} , its nucleophilic nature,^{7, 11} and its tendency to bridge,¹²⁻¹⁶ only a handful of molecules displaying terminally bound Nb nitrides are known.¹⁷⁻²⁰ Cummins and co-workers reported three examples of anionic niobium nitrides (Fig. 1, left), all of which derive from reductive routes using Nb^{IV} precursors such as $\text{ClNb}(\text{N}[\text{R}]\text{Ar})_3$ ($\text{R} = ^t\text{Bu}, ^i\text{Pr}, \text{CH}_2^t\text{Bu}$) by either splitting N_2 using heterobimetallic systems^{18, 20} or via decarbonylation of isocyanate.¹⁷ In an interesting twist, Arnold

and co-workers found access to a zwitterionic Nb nitride (Fig. 1, center) by taking advantage of a photochemically driven process where the Nb^{V} does not formally change oxidation state during the reaction.¹⁹ Instead, their strategy involves photochemically promoting N_2 extrusion from a $\text{Nb}^{\text{V}}\text{-N}_3$, with the required $2e^-$ equivalents coming from the reductive coupling of Nb -phenyl and $\text{Nb}=\text{N}^t\text{Bu}$ moieties to form an anilide $\text{Nb}-\text{N}^t\text{BuPh}$ (Fig. 1). In other words, the ligands provide the $2e^-$ needed to achieve the reductive splitting of N_3^- into N^{3-} and N_2 . Unfortunately, this procedure relies on a borane $\text{B}(\text{C}_6\text{F}_5)_3$ to cap and trap the elusive neutral nitride ligand, resulting in the formation of a zwitterionic nitrido borate and not a truly terminal nitride.¹⁹

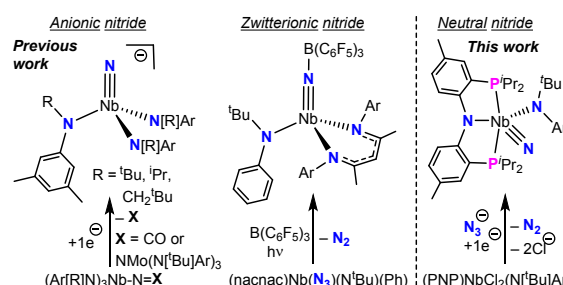


Fig. 1 Examples of structurally characterized anionic and zwitterionic mononuclear Nb nitrides (previous studies) along with the neutral and terminal Nb nitride reported in this work.

These two distinct routes share in common the use of hard nitrogen donors to stabilize the nitrido ligand as well as the necessity of a transient and highly reducing Nb^{III} ion. Learning from these approaches we hypothesized that an anilide was not only an ideal ligand to stabilize a nitride, but that the ubiquitous N_3^- could be the nitride source under reducing conditions, while also taking advantage of a redox-active ligand based on our recent finding that a neutral and terminal phosphide ligand can be assembled on Nb using the redox-active $[\text{PNP}]^-$ ligand.²² Recently, we found that the pincer ligand $[\text{PNP}]^-$ was indeed suitable for stabilizing the methylidyne $(\text{PNP})\text{Nb}\equiv\text{CH}(\text{OAr})$ ($\text{Ar} = \text{2,6-}i\text{Pr}_2\text{C}_6\text{H}_3$) and that such system could undergo cross-metathesis with NC^tBu or NCAd to form $(\text{PNP})\text{Nb}\equiv\text{N}(\text{OAr})$ and

[a] Department of Chemistry, University of Pennsylvania, Philadelphia, PA 19104 (USA). E-mail: mindiola@sas.upenn.edu

[b] Department of Chemistry, Korea Advanced Institute of Science and Technology (KAIST), Daejeon 34141, Republic of Korea. E-mail: mbaik2805@kaist.ac.kr

[c] Center for Catalytic Hydrocarbon Functionalizations, Institute for Basic Science (IBS), Daejeon 34141, Republic of Korea.

† Electronic supplementary information (ESI) available. CCDC xxxxx. For ESI and crystallographic data in CIF or other electronic format see DOI: 10.1039/x0xx00000x

the terminal alkyne.²¹ Despite performing ¹⁵N isotopic labeling studies for the neutral nitride, we were unable to crystallographically characterize and unambiguously confirm its terminal nature. This feature along with the multistep process required to make its methylidyne precursor rendered this approach synthetically cumbersome. Hence, in order to stabilize a terminal and neutral nitride on Nb, a square pyramidal geometry seemed appropriate to use. In this work we show how the Nb^{IV} precursor (PNP)NbCl₂(N^tBu)Ar²² (**1**) can be the source of a terminal and neutral nitride ligand directly from azide reduction and we establish that the PNP ligand plays a crucial redox-active role, whereas the anilide ligand assists the N-atom transfer to Nb. Independent synthetic routes in combination with computational studies were used to probe the mechanism of formation of the neutral nitride ligand on Nb^V, which was spectroscopically and structurally characterized including ¹⁵N enriched isotopic labelling studies.

Recently, we reported the formation of complex **1** from the transmetallation of (PNP)NbCl₃ and Li(N^tBu)Ar.²² When **1** was treated with one equiv of NaN₃ in THF over 16 h, two diamagnetic Nb compounds were observed in approximately 1:1 ratio based on a combination of ¹H and ³¹P NMR spectral studies (Fig. S16 and Fig. S17). The ¹H NMR spectrum also revealed two C₁-symmetric complexes in solution. Notably, the ³¹P NMR spectrum shows one compound to contain an intact PNP ligand (two broad phosphorus environments at 35.36 and 36.58 ppm) whereas the second species has two distinct phosphorus doublets at 41.57 and 11.83 ppm with *J*_{PP} = 44 and 40 Hz respectively (Fig. S17). Despite unsatisfactory combustion analysis,^{23, 24} full NMR spectral characterization, and fractional crystallization from a pentane solution followed by a single crystal X-ray diffraction study (sc-XRD) allowed for the identification of these two species as (PNPN)NbCl₂(N^tBu)Ar (**2**) and (PNP)Nb≡N(N^tBu)Ar (**3**) in 56% combined yield²⁴ as shown in Fig. 2 and Scheme 1. Whereas the structural study (Fig. 2) confirmed oxidation of one P-arm of the PNP ligand and transoid orientation of the two Cl⁻ in the case of **2**, complex **3** represents the first example of a terminal and neutral Nb nitrido complex with a short Nb≡N bond length of 1.698(2) Å.^{18, 20} For **2**, the Nb center resides in a highly distorted octahedral geometry, while for **3** the geometry value is more in accord with a square pyramidal structure (*τ*₅ = 0.03)²⁵ akin to what was observed for (PNP)Nb≡CH(OAr) (*τ*₅ = 0.03).²¹ The ¹⁵N NMR spectrum of the ¹⁵N enriched **2**-¹⁵N has a resonance at 351 ppm (*Δ**v*_{1/2} = 11 Hz) while **3**-¹⁵N has a further downfield resonance at 824 ppm (*Δ**v*_{1/2} = 10 Hz; referenced to AdCN at 242 ppm vs. NH₃(l) at 0 ppm).

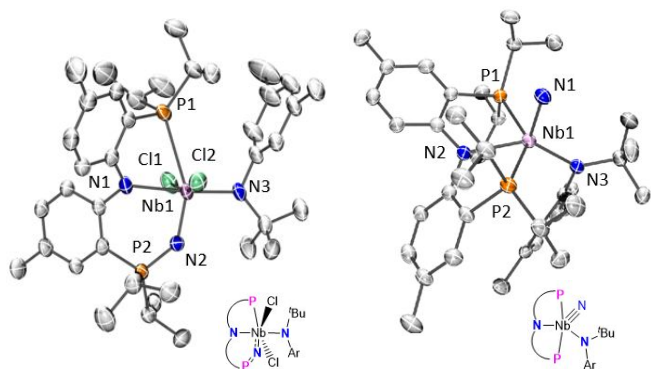
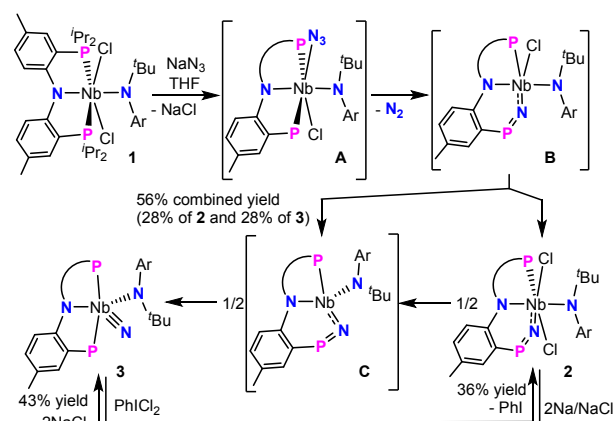


Fig. 2 Molecular structures of complexes **2** (left) and **3** (right) with thermal ellipsoids at the 50% probability level and their line drawings below. All hydrogen atoms and co-crystallized pentane from **2** have been omitted for clarity.

Despite having similar solubilities, compound **2** recrystallizes first after workup from a concentrated pentane solution at -35 °C. Further recrystallization of the pentane supernatant allows for the isolation of **3**. Compounds **2** and **3** are likely formed from an initial transmetallation step to produce [(PNP)NbCl(N₃(N^tBu)Ar)] (**A**), followed by N₂ ejection and ligand oxidation to form the phosphinimide [(PNPN)NbCl(N^tBu)Ar)] (**B**). Disproportionation of **B** most likely produces **2** and the unstable Nb^{III} species [(PNPN)Nb(N^tBu)Ar)] (**C**), which intramolecularly splits the P=N bond to form the nitrido complex **3** as outlined in Scheme 1. Since a disproportionation step relates **2** and **3**, we decided to chemically reduce **2** by two e⁻ via putative intermediate **C** to the terminal nitride **3**, in as much as oxidize the nitride **3** by the same amount of e⁻ to promote PNP oxidation to yield the phosphinimide-dichloride complex **2**.

Accordingly, chemical reduction of **2** using 2 equiv Na/NaCl resulted in the formation of **3** in 43% yield along with some PNP and NaPNP that was confirmed by ³¹P and ¹H NMR spectroscopy (Fig. S18 and Fig. S21).²⁴ Similarly, chemical oxidation of **3** with PhICl₂ formed **2** in 36% yield along with other intractable side products (Fig. S19 and Fig. S23).²⁴



Scheme 1 Synthesis of complexes **2** and **3** and proposed mechanism.

We used density functional theory calculations at the B3LYP-D3/cc-pVTZ(-f)/LACV3P//6-31G**/LACVP level of theory²⁶⁻³³ to gain further insight into the detailed mechanism of formation of **2** and **3** (see Supporting Information for details) and understand the differing reactivity of **1** with the analogous P-atom transfer reagent, NaOCP²² (Fig. S29). As illustrated in Fig. 3, the reaction begins with the transmetallation step resulting in the azide-bound complex **A**. N₂ release from **A** results in the cation radical complex **D** and traverses the transition state **A-TS** which involves three consecutive intramolecular electron transfer steps (Fig. S24–S27) to afford a barrier of 24.0 kcal/mol. The highly exergonic N₂ release step and the redox non-innocent nature of the PNP ligand enables the formation of **D** with a strong Nb–N bond, thus rendering it to be a cation radical, which is 31.4 kcal/mol lower in energy than **A**. The following N–

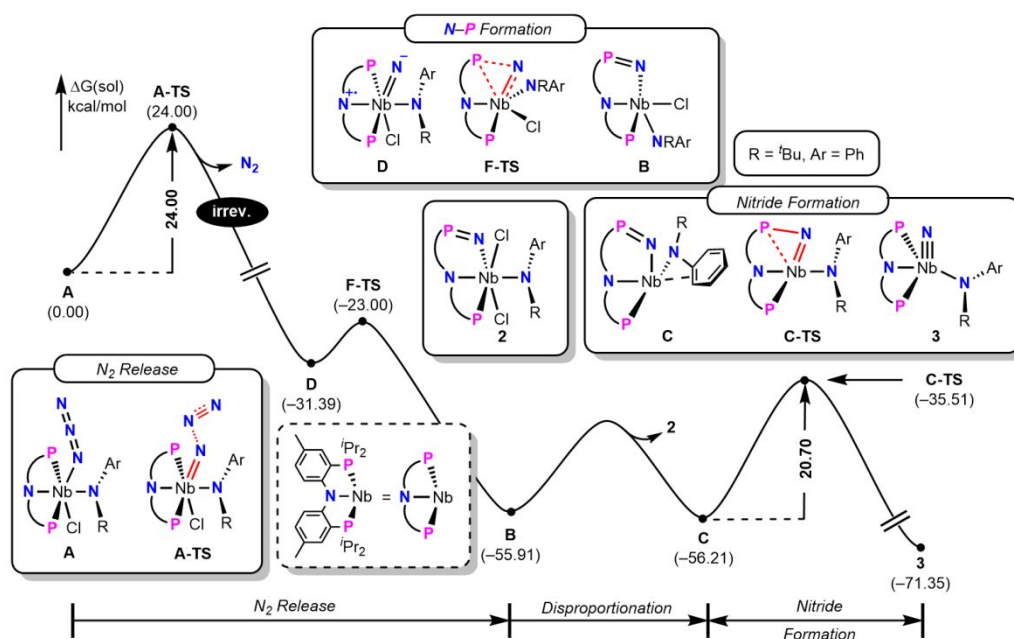


Fig. 3 Solvation-corrected Gibbs free energy profile for the conversion of **A** into **2** and **3**.

P bond formation (**F-TS**) from **D** involves energetically low isomerization steps between the anilide and the chloride ligand (Fig. S28). The resulting intermediate **B** undergoes thermoneutral disproportionation to form **2** and **C**. As shown in Fig. 3, the anilide aryl plays a crucial role (Fig. S30) in stabilizing the intermediate **C** and in facilitating the complete intramolecular N-atom transfer from P to Nb via **C-TS** to form the nitride **3** with a barrier of 20.7 kcal/mol.

In summary, we show that the redox active ligand is critical for assembling the neutral and terminal niobium nitride and it can be directly accessed using NaN_3 as the N-atom source. Theoretical studies suggest that the initial transmetallation followed by N_2 release forms an unprecedented anionic niobium nitride with a ligand centered radical cation, whereby the redox non-innocent character of the pincer ligand drives the reaction to be highly exergonic. The following ligand-assisted coupling of the nitride affords Nb^{IV} phosphinimide, which undergoes disproportionation to yield the fully characterized Nb^{V} phosphinimide and the reducing Nb^{III} phosphinimide intermediate. Finally, reductive decoupling of the P–N bond of the Nb^{III} phosphinimide, via assistance from the anilide ligand, furnishes the fully characterized neutral Nb^{V} nitride. Further reactivity studies disclose that P–N bond formation is promoted upon $2e^-$ oxidation of the nitride whereas Nb^{V} nitride formation can be accomplished via $2e^-$ reduction of **2**.

For funding, we thank the University of Pennsylvania and the U. S. National Science Foundation (NSF; Grants CHE-0848248 and CHE-1152123) and the Institute for Basic Science in Korea for financial support (IBS-R010-A1).

Conflicts of interest

There are no conflicts to declare.

Notes and references

- S. T. Oyama, *Introduction to the chemistry of transition metal carbides and nitrides*, Springer, Dordrecht, 1996.
- C. Angelkort, H. Lewalter, P. Warbichler, F. Hofer, W. Bock and B. O. Kolbesen, *Spectrochim. Acta A Mol. Biomol. Spectrosc.*, 2001, **57**, 2077–2089.
- A. Kafizas, C. J. Carmalt and I. P. Parkin, *Coord. Chem. Rev.*, 2013, **257**, 2073–2119.
- T. Nguyen, A. Tavakoli, S. Triqueneaux, R. Swami, A. Ruhtinas, J. Gradel, P. Garcia-Campos, K. Hasselbach, A. Frydman, B. Piot, M. Gibert, E. Collin and O. Bourgeois, *J. Low Temp. Phys.*, 2019, **197**, 348–356.
- S. Volkov, M. Gregor, T. Roch, L. Satrapinsky, B. Grančič, T. Fiantok and A. Plecenik, *J. Electr. Eng.*, 2019, **70**, 89–94.
- G. Yang, X. Zhao, F. Liao, Q. Cheng, L. Mao, H. Fa and L. Chen, *Sustain. Energy Fuels*, 2021, **5**, 3039–3083.
- B. L. Tran, M. Pink, X. Gao, H. Park and D. J. Mindiola, *J. Am. Chem. Soc.*, 2010, **132**, 1458–1459.
- M. E. Carroll, B. Pinter, P. J. Carroll and D. J. Mindiola, *J. Am. Chem. Soc.*, 2015, **137**, 8884–8887.
- L. N. Grant, B. Pinter, J. Gu and D. J. Mindiola, *J. Am. Chem. Soc.*, 2018, **140**, 17399–17403.
- R. Thompson, C. H. Chen, M. Pink, G. Wu and D. J. Mindiola, *J. Am. Chem. Soc.*, 2014, **136**, 8197–8200.
- L. N. Grant, B. Pinter, T. Kurogi, M. E. Carroll, G. Wu, B. C. Manor, P. J. Carroll and D. J. Mindiola, *Chem. Sci.*, 2017, **8**, 1209–1224.
- A. Caselli, E. Solari, R. Scopelliti, C. Floriani, N. Re, C. Rizzoli and A. Chiesi-Villa, *J. Am. Chem. Soc.*, 2000, **122**, 3652–3670.
- M. D. Fryzuk, C. M. Kozak, M. R. Bowdridge, B. O. Patrick and S. J. Rettig, *J. Am. Chem. Soc.*, 2002, **124**, 8389–8397.
- F. Akagi, T. Matsuo and H. Kawaguchi, *Angew. Chem. Int. Ed. Engl.*, 2007, **46**, 8778–8781.
- A. J. Keane, B. L. Yonke, M. Hirotsu, P. Y. Zavalij and L. R. Sita, *J. Am. Chem. Soc.*, 2014, **136**, 9906–9909.
- K. Searles, P. J. Carroll, C. H. Chen, M. Pink and D. J. Mindiola, *Chem. Commun.*, 2015, **51**, 3526–3528.
- M. G. Fickes, A. L. Odom and C. C. Cummins, *Chem. Commun.*, 1997, DOI: 10.1039/a704253a, 1993–1994.

- 18 D. J. Mindiola, K. Meyer, J.-P. F. Cherry, T. A. Baker and C. C. Cummins, *Organometallics*, 2000, **19**, 1622–1624.
- 19 C. Camp, L. N. Grant, R. G. Bergman and J. Arnold, *Chem. Commun.*, 2016, **52**, 5538–5541.
- 20 J. S. Figueroa, N. A. Piro, C. R. Clough and C. C. Cummins, *J. Am. Chem. Soc.*, 2006, **128**, 940–950.
- 21 T. Kurogi, P. J. Carroll and D. J. Mindiola, *J. Am. Chem. Soc.*, 2016, **138**, 4306–4309.
- 22 S. Senthil, S. Kwon, D. Fehn, H. Lim, M. R. Gau, P. J. Carroll, M.-H. Baik and D. J. Mindiola. *Manuscript submitted for publication*.
- 23 F. P. Gabbaï, P. J. Chirik, D. E. Fogg, K. Meyer, D. J. Mindiola, L. L. Schafer, and S.-L. You, *Organometallics*, 2016, **35**, 3255–3256.
- 24 See Supporting Information.
- 25 A. W. Addison, T. N. Rao, J. Reedijk, J. van Rijn and G. C. Verschoor, *J. Chem. Soc., Dalton Trans.*, 1984, 1349–1356.
- 26 J. C. Slater, *Quantum Theory of Molecules and Solids, Vol. 4: The Self-Consistent Field for Molecules and Solids*. McGraw-Hill: New York, 1974.
- 27 S. H. Vosko, L. Wilk and M. Nusair, *Can. J. Phys.*, 1980, **58**, 1200–1211.
- 28 A. D. Becke, *Phys Rev A Gen Phys*, 1988, **38**, 3098–3100.
- 29 C. Lee, W. Yang and R. G. Parr, *Phys Rev B Condens Matter*, 1988, **37**, 785–789.
- 30 S. Grimme, J. Antony, S. Ehrlich and H. Krieg, *J. Chem. Phys.*, 2010, **132**, 154104.
- 31 P. J. Hay and W. R. Wadt, *J. Chem. Phys.*, 1985, **82**, 270–283.
- 32 W. R. Wadt and P. J. Hay, *J. Chem. Phys.*, 1985, **82**, 284–298.
- 33 P. J. Hay and W. R. Wadt, *J. Chem. Phys.*, 1985, **82**, 299–310.